27th EPS Conference on Contr. Fusion and Plasma Phys. Budapest, 12-16 June 2000 ECA Vol. **24B** *(2000) 1421 -1424*

Radial and Poloidal Impurity Transport in the H-mode Edge Pedestal of Alcator C-Mod

T. Sunn Pedersen*, R. Granetz, A. Hubbard, E. Marmar,
D. Mossessian, J. Hughes, I. Hutchinson, J. Rice, J. Terry
MIT Plasma Science and Fusion Center, Cambridge, MA 02139, USA
**Present address: Dept. of Applied Physics, Columbia University, New York, NY 10027, USA*

Abstract

Radial impurity density profiles in the H-mode edge pedestal region of Alcator C-Mod have been quantitatively derived from very high-resolution ($dR \sim 1-2$ mm) measurements of $n_e(r)$, $T_e(r)$, and x-ray emissivity of fluorine at two poloidal locations (outboard midplane and top). At the midplane, the observed inward shift of the fluorine density (n_F) pedestal with respect to the n_e pedestal is found to be consistent with the neoclassical pinch velocity, both in magnitude and spatial structure. The empirically observed dependencies of the soft x-ray emissivity pedestal width on plasma parameters and H-mode type are shown to be indicative of changes in the impurity diffusion coefficient, D_I, at the plasma edge. The soft x-ray pedestal profile at the top of the plasma varies considerably from that at the midplane, implying that impurity density is not constant on flux surfaces. Specifically, the top n_F pedestal is close to the separatrix, unlike the midplane pedestal. An accumulation of impurities at the top of the plasma could, in principle, explain this difference, and is qualitatively consistent with the neoclassically predicted Pfirsch-Schlüter return flow in the pedestal region in response to the ion ∇B drift.

1. Introduction

The high confinement mode (H-mode) [1] is an attractive confinement mode for a future fusion reactor, because of the increase of a factor of $\sim$2 in energy confinement time compared to the low confinement mode (L-mode), observed in diverted tokamak experiments. However, the impurity confinement time also increases, often by more than an order of magnitude, which leads to impurity accumulation, and a resulting degradation of fusion performance due to increased radiation losses and fusion fuel dilution. Fortunately, several types of H-modes have been discovered (for instance, the ELMy H-mode, and the EDA H-mode [2]) which have a somewhat lower impurity confinement time, allowing for good quality, steady state H-modes. The H-mode is characterized by a narrow region of greatly improved confinement near the separatrix. This region is called the edge transport barrier region, or edge pedestal region. A better understanding of the physics of this region is important in order to predict H-mode performance in future devices. Alcator C-Mod, which is a shaped, high magnetic field, high plasma density tokamak, has particularly narrow H-mode transport barriers, typically less than 1 cm. In recent years, a number of high resolution edge diagnostics have been installed, leading to a much improved coverage of the edge region. At the top of the plasma soft x-ray emissivity profiles are measured with 1.2 mm radial resolution, and a Thomson scattering diagnostic measures T_e and n_e

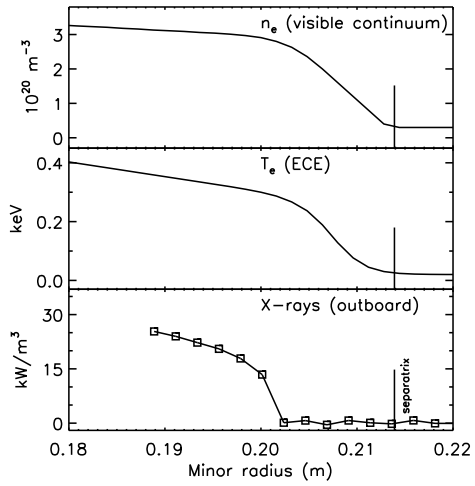

Figure 1: *Edge profiles of $n_e(r)$, $T_e(r)$, and $X(r)$ near the outboard midplane for an ELM-free H-mode. The x-ray pedestal is significantly narrower and further into the plasma than the T_e and n_e pedestals.*

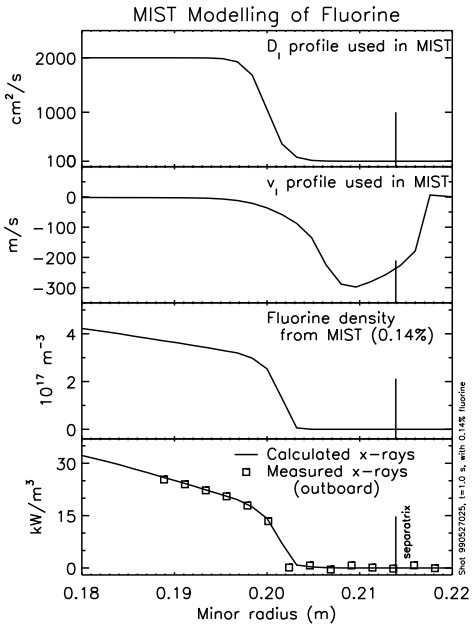

Figure 2: *Radial profiles $D_I(r)$, and $v_I(r)$ with the resulting $n_F(r)$, and $X_{sim}(r)$, closely resembling $X(r)$.*

profiles with 1 mm radial resolution. At the outboard edge, near the midplane, a visible continuum diagnostic measures $n_e Z_{eff}$ with 2.5 mm resolution, a second soft x-ray array measures soft x-ray emissivity with 1.5 mm resolution, and an ECE diagnostic measures T_e profiles with approximately 9 mm resolution. These diagnostics are described in Ref. [3]-[5]. Measurements from the three diagnostics at the outboard edge have been used to derive impurity transport coefficients in the H-mode transport barrier. This is described in Section 2. The simultaneous measurements of soft x-ray emissivity in two poloidally separate locations allow us to extract information about the poloidal structure of the soft x-ray emissivity. Contrary to what is usually assumed, we measure large poloidal variations in soft x-ray emissivity in the H-mode transport barrier region, implying a strong poloidal variation in impurity density. These results are discussed in Section 3.

2. Radial transport

Given well-resolved profiles of T_e, n_e, and soft x-ray emissivity, absolutely calibrated profiles of fluorine density n_I can be obtained together with profiles of the impurity transport coefficients D_I (diffusion coefficient) and v_I (convective, or 'pinch' velocity). The procedure, described in detail in Ref. [6], is as follows. The measured profiles of $T_e(r)$ and $n_e(r)$, together with initial guesses for $D_I(r)$, and $v_I(r)$, and the core fluorine density $n_F(r=0)$ are used as inputs to the impurity transport code MIST [7]. This code calculates the steady state density profiles for all charge states of a specified impurity species, in this case fluorine. Given the charge state density profiles and the profiles of T_e and n_e, recombination and line emission rates are calculated for each radial location, and the resulting emissivity spectrum is convolved with the beryllium filter function to finally yield a simulated soft x-ray emissivity profile $X_{sim}(r)$ which can be directly compared to the measured soft x-ray emissivity profile $X(r)$. The input $D_I(r)$,

$v_I(r)$, and $n_F(r=0)$ are then varied to minimize $|X(r) - X_{sim}(r)|$. Using the outboard edge x-ray emissivity just above the midplane, T_e from ECE at the midplane and n_e from the visible continuum diagnostic just below the midplane, we have determined radial transport coefficients and density profiles for fluorine. The proximity of all three measurements to the outboard midplane eliminates field line mapping uncertaincies. An example of a set of measured H-mode profiles is shown in Figure 1, and the corresponding profiles of D_I, v_I, and n_F are shown together with a comparison between $X(r)$ and $X_{sim}(r)$ in Figure 2. The v_I profile was chosen to be equal to the neoclassical impurity pinch [8], calculated assuming $T_i(r) = T_I(r) = T_e(r)$, and $n_i(r) = n_e(r)$. As can be seen, excellent agreement between $X(r)$ and $X_{sim}(r)$ is found. The $n_F(r)$ profile shapes are very similar to the $X(r)$ shapes, showing a distinct, narrow pedestal, located further into the plasma than the $n_e(r)$ pedestal. This inward shift is caused by the large inward convection in the region of large plasma density gradient, as predicted by the neoclassical theory. In general, our results are consistent with neoclassical theory, and a strong inward pinch is always present, localized to the region of large density gradient (as measured by the visible continuum diagnostic). The width of the $X(r)$ pedestal (and of the $n_F(r)$ pedestal) is determined mostly by the value of $D_I(r)$ in the H-mode pedestal region, D_I^H. Thus, previously published scalings of $X(r)$ pedestal widths in EDA H-mode[4], can be interpreted as scalings of D_I^H. We conclude that D_I^H is a strongly decreasing function of plasma current in EDA H-mode, varying from $D_I^H = 500 - 1000$ cm^2/s at $I_p = 0.8$ MA, to $D_I^H = 100 - 200$ cm^2/s at $I_p = 1.2$ MA. We also conclude that D_I^H increases with increasing triangularity, and is affected by the sign of dI_p/dt. In ELM-free H-modes, where the x-ray pedestal width is only 1.5-3 mm, we find that $D_I^H = 50 - 100$ cm^2/s, consistent with independent estimates of D_I^H [9]. No clear scalings have been identified in ELM-free H-modes. This may be due to insufficient radial resolution, as the soft x-ray pedestals normally are 1.5-3 mm wide, only barely resolved with the 1.5 mm resolution.

3. Poloidal asymmetries

The two simultaneous measurements of the soft x-ray emissivity in poloidally separate locations enables us to measure poloidal variations in the soft x-ray emissivity in the edge region of the plasma. Indeed, a large poloidal asymmetry is seen in H-mode. Clear x-ray emissivity pedestals are always observed during H-mode in both locations, but the pedestals at the top of the plasma are located within a few mm of the separatrix, whereas the soft x-ray pedestal at the outboard plasma edge is typically 10 mm inside the nominal EFIT separatrix. There are some indications that the real separatrix is 3-6 mm radially inward of the EFIT separatrix at the midplane, (but presumably is accurate at the top of the plasma) which therefore would explain part, but not all of the difference in the X(r) pedestal locations. The pedestal widths can differ significantly too. The largest differences in pedestal widths are seen in low current ($I_p \approx 0.8$ MA), high edge q ($q_{95} \approx 5.5$) EDA H-modes, where the x-ray pedestal width at the outboard edge is typically 5 mm, but only 2 mm at the top of the plasma. Width differences of a factor of 2.5 cannot be caused by uncertainties in the EFIT magnetic reconstruction, since this would imply that there is no flux expansion from the outboard edge to the top of the plasma. The flux expansion is about 2.5 in typical Alcator C-Mod plasmas. The differences in pedestal location and width both increase with q_{95}, as seen in Figures 3 and 4. The asymmetries we observe imply that the soft x-ray emissivity is much larger at the top of a particular flux surface than at the outboard edge. Since the electron density and temperatures can equilibrate very quickly along field lines, we are led to conclude that the impurity (fluorine) particles tend to accumulate at the top of the flux surfaces near the plasma edge. Large parallel gradients in

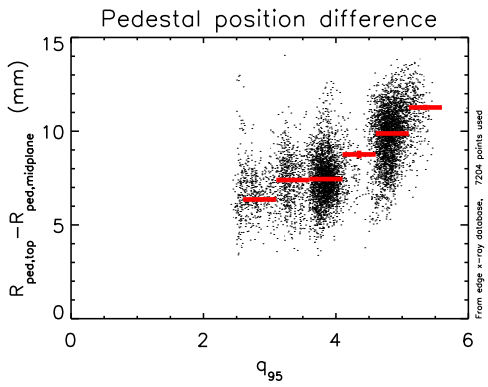

Figure 3: *The difference in x-ray pedestal location increases with q_{95}. The red bars indicate binned averages.*

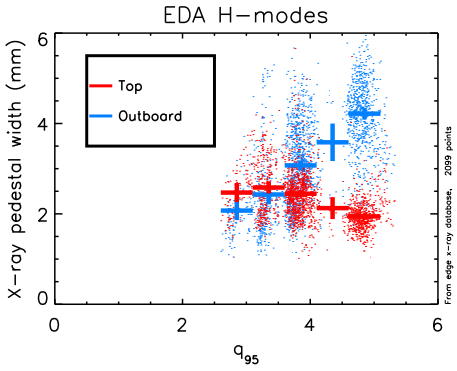

Figure 4: *The x-ray pedestal width increases with q_{95} at the outboard edge in EDA H-mode, but has a decreasing trend at the top.*

impurity density could be driven by collisional friction with the bulk ion Pfirsch-Schlüter return flow caused by the ion ∇B drift. If this is the case, then the asymmetry should change sign when the field direction is reversed. Experiments for reversed field H-modes with lower x-point are planned to test this explanation. Large up-down asymmetries in argon density have previously been seen in Alcator C-Mod [10]. The asymmetry did change sign when the ∇B drift direction was reversed, supporting the present explanation. Although various neoclassical theories have shown that an up-down impurity asymmetry should exist, none of them predict as large asymmetries as we have observed. This may be due to the fact that in Alcator C-Mod H-modes, the density gradient scale lengths are on the order of the ion poloidal gyroradius, which makes an accurate analytical treatment very difficult. In addition, the timescales for radial and poloidal equilibration are comparable. It is usually assumed that the poloidal equilibration time is faster than the radial equilibration time. It may be necessary to use two-dimensional computer simulations to accurately capture the complex dynamics at the plasma edge.

References

[1] F. Wagner et *al.*, Phys. Rev. Letters **49**, p. 1408 (1982)
[2] M. Greenwald et *al.*, Phys. Plasmas, **6**, p. 1943, (1999)
[3] D. Mossessian et *al.*, Plasma Phys. Contr. Fusion **42**, A255-A262
[4] T. Sunn Pedersen and R.S. Granetz, Rev. Sci. Instrum. **70** (1999), p. 586
[5] T. Sunn Pedersen and R.S. Granetz, "Simultaneous soft x-ray emissivity profile measurements in poloidally separate locations of the Alcator C-Mod edge plasma", accepted in Rev. Sci. Instrum., May 2000
[6] T. Sunn Pedersen et *al.*, "Radial Impurity Transport in the H-Mode Transport Barrier Region in Alcator C-Mod", submitted to Nucl. Fusion (March 2000)
[7] R.A. Hulse, Nuclear Technology/Fusion **3** (1983) p. 259
[8] P.H. Rutherford, Phys. Fluids **17** (1974), p. 1782
[9] J.E. Rice et *al.*, Phys. Plasmas **4** (1997), p. 1605
[10] J.E. Rice et *al.*, Nucl. Fusion **37** (1997), p. 241